ChemComm

Cite this: *Chem. Commun.*, 2012, **48**, 1889–1891

www.rsc.org/chemcomm

COMMUNICATION

Absorption enhancement of oligothiophene dyes through the use of a cyanopyridone acceptor group in solution-processed organic solar cells†

Akhil Gupta,[ab] Abdelselam Ali,[a] Ante Bilic,[c] Mei Gao,[a] Katalin Hegedus,[a] Birendra Singh,[a] Scott E. Watkins,*[a] Gerard J. Wilson,[a] Udo Bach[b] and Richard A. Evans*[a]

Received 23rd November 2011, Accepted 5th December 2011
DOI: 10.1039/c2cc17325e

Improvements in the performance of small molecule-based organic solar cells have been reported through the use of a cyanopyridone acceptor group. This acceptor fragment enhances the absorbance of an oligothiophene-based dye and enables the addition of a solubilising alkyl chain that facilitates simple device fabrication from solution.

Organic photovoltaic devices are an emerging technology that have the potential to deliver significant benefits and cost savings in comparison with solar cells based on traditional, inorganic semiconductors.[1] Recent reports of improving device performances using small molecule organic semiconductors has attracted some attention away from the study of more established polymeric semiconductors such as poly(3-hexylthiophene) (P3HT).[2,3] To date, devices with power conversion efficiencies of over 5% have been reported using small molecules as active materials.[4] From a synthetic point of view, small molecules offer potential advantages over polymeric materials in terms of ease of synthesis and purification and suffer less from batch to batch variations and end group contamination. Intermolecular associations, which can assist with charge transport, are also typically stronger in small molecules than in polymeric materials.[5]

A key advantage of organic semiconductors is that they typically have high absorption coefficients ($>10^4$ cm^{-1}). This property compensates for the low charge mobilities typically observed in organic semiconductors by enabling efficient light absorption and charge collection within thin films (<200 nm). One successful strategy to improve the performance of small molecule organic materials has been the design of donor–acceptor compounds that show charge transfer absorption. Key examples of this approach include the merocyanine colourants reported by Meerholtz *et al.*,[6,7] the diketopyrrolopyroles reported by Nguyen *et al.*[2,8] and the oligothiophenes reported by Bäuerle *et al.*[9] A recent review highlighted the potential improvements to the absorption properties and the energy level alignment between various donor and acceptor fragments through the use of charge transfer absorption.[10] There is, therefore, considerable synthetic interest in exploring new donor–acceptor combinations and in making molecules that can be processed from solution. In this communication, we report a design strategy to explore both areas.

In this study, we chose an oligothiophene with a triarylamine end-group as the donor component in our small molecules (see Fig. 1). Oligothiophenes have been reported in highly efficient devices by Bäuerle *et al.*[9] and a similar triarylamine-based donor unit has been previously reported by Wong *et al.*[11] For both classes, a dicyanovinyl acceptor group has commonly been used. In addition, all of these studies have been of devices prepared by vacuum deposition. In order to vary the electronic and optical properties and the processability of the small molecules, we introduced a cyanopyridone fragment as the acceptor group, see compound **1** in Fig. 1. When compared with the commonly used dicyanovinylidene group (compound **2**, Fig. 1) the aromatisable ethylhexylcyanopyridone is an acceptor of greater strength. Compound **1** can have a variety of canonical forms contributing to its electronic structure. In one form, the cyanopyridone may be aromatized to give a zwitterionic resonance form of **1** (see Fig. S2 in ESI†). The combination of electron-donating amine and aromatizable acceptors, of which cyanopyridone is an example, is a common strategy in non-linear dye design and provides

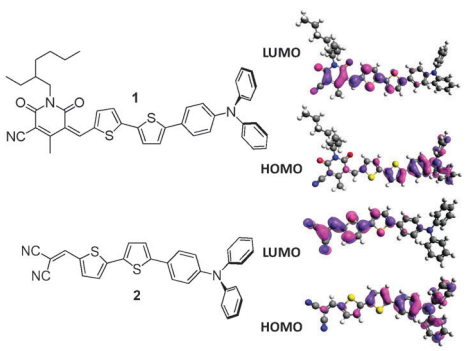

Fig. 1 Molecular structures and calculated orbital densities of the HOMO and LUMO for compounds **1** and **2**.

[a] *CSIRO Materials Science and Engineering, Flexible Electronics Theme, Bayview Avenue, Clayton South, 3169, Victoria, Australia. E-mail: scott.watkins@csiro.au, richard.evans@csiro.au; Fax: +61395452446; Tel: +61395452507*
[b] *Department of Materials Engineering, Monash University, Wellington Road, Clayton 3800 Victoria, Australia*
[c] *CSIRO Mathematics Informatics and Statistics, Bayview Avenue, Clayton 3169, Victoria, Australia*

† Electronic supplementary information (ESI) available: Detailed synthetic protocols, scalable synthetic strategy, DFT calculations, cyclic-voltammograms, thin film absorption spectra, device fabrication details. See DOI: 10.1039/c2cc17325e

large red shifts of lamda maxima over conventional acceptors like dicyanovinylidene. Density Functional Theory calculations using the Gaussian 03 suite of programs[12] show a more polar distribution of the orbital density in the HOMO for compound **1** as compared with compound **2** (see Fig. 1). For both compounds **1** and **2**, the electron density of the LUMO is mainly localised on the acceptor part. An additional advantage of the cyanopyridone acceptor unit is that a variety of alkyl groups can be located on the nitrogen atom and so allow tuning of solubility. In the present case, the ethylhexyl group was the substituent of choice for producing high solubility and excellent film forming properties without crystallisation occurring in the film.

The materials **1** and **2** were synthesised from 5′-(4-(diphenylamino)phenyl)-2,2′-bithiophene-5-carbaldehyde, by reaction with 1-(2-ethylhexyl)-4-methyl-2,6-dioxo-1,2,5,6-tetrahydropyridine-3-carbonitrile in methanol at reflux to yield compound **1** and with malononitrile, in chloroform at reflux with pyridine as base, to yield the analogue compound **2**. Of particular note is the fact that the synthesis of compound **1** was scaled-up to give material with higher purity (as measured by HPLC) with no chromatographic purification or crystallisation required in any step (for scaled-up synthesis details see Fig. S1 in ESI†). The synthesis of multi-gram quantities of pure materials without requiring chromatography is a significant result. These new materials were prepared in moderate to high yields and all the synthetic and characterisation details are described in ESI†.

The ultraviolet-visible (UV-Vis) spectral absorptivities of both the materials were measured in chloroform solution and are represented in Fig. 2. As predicted, the stronger acceptor group, cyanopyridone, induces a strong red-shift in the absorption of compound **1** compared with the dicyanovinyl group. An absorption maximum at 590 nm (ε = 61 028 M^{-1} cm^{-1}) with the onset at 722 nm were measured for compound **1**, and an absorption maximum at 514 nm (ε = 41 249 M^{-1} cm^{-1}) with an onset at 636 nm were measured for compound **2**. With increased acceptor strength, we found a 50% enhancement to the peak molar absorptivity of compound **1** compared with compound **2**. Of particular relevance, we observe the same bathochromic absorption shift in thin film spectra of compound **1** compared with compound **2** (see Fig. S3 in ESI†).

The HOMO energies of compounds **1** and **2** were estimated using Photo Electron Spectroscopy in Air (PESA) and the LUMO energies were calculated by adding the bandgap to the HOMO values, see Table 1. The UV-Vis spectra show that the

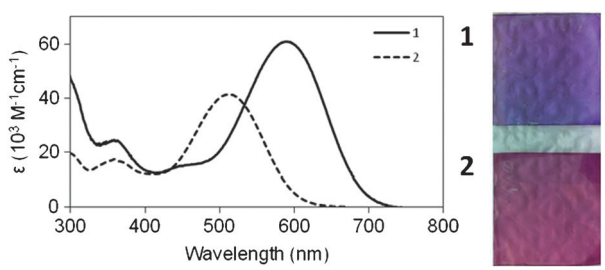

Fig. 2 Molar absorptivities of compounds **1** and **2** in chloroform solutions (left) and photographic images of thin films of compounds **1** and **2** (right).

cyanopyridone acceptor reduces the band gap of compound **1** as compared with compound **2**. This is in agreement with the calculated energy levels (see Fig. S4 in ESI†). Electrochemistry experiments show that while the reduction processes are irreversible both the compounds undergo two, reversible oxidation processes (Fig. S5 in ESI†), thus emphasising their suitability as *p*-type materials in solar cells. The photo-physical and electronic properties of compounds **1** and **2** are summarised in Table 1.

An initial screen of efficacy of the target compound, **1**, as a *p*-type material in a solar cell was carried out by using it in a planar heterojunction device. The use of this device structure, with single component layers, enables materials to be evaluated independently of the effects of film morphology that can be complex in a two component blend. Compound **1** was deposited from solution as a pristine layer and the remainder of the device was fabricated by vacuum deposition. Planar heterojunction devices using C_{60} as the electron acceptor and bathocuproine (BCP) as the exciton blocking layer were fabricated. Devices with the structure ITO/PEDOT:PSS (38 nm)/**1**/C_{60} (20–35 nm)/BCP (10 nm)/Al (100 nm) gave a maximum power conversion efficiency of 1.29% (see Section 7.1 in ESI†), a result that is comparable with other recently reported oligothiophenes in evaporated devices.[9] This efficiency increased with a decrease in thickness of compound **1**. This suggests that the inherent charge mobility of this film is the limiting factor rather than the absorbance. This observation is also consistent with the low mobilities measured for these compounds, albeit in a different (OFET) configuration (see Table S6 in ESI†).

Having established that compound **1** performed as a *p*-type material in OPVs, a direct comparison with the dicyanovinyl analogue in a solution-processed, bulk heterojunction (BHJ) device was carried out. BHJ architectures typically deliver higher device power conversion efficiencies by maximising the surface area of the interface between the *p*- and *n*-type materials in the active layer. For both compounds, the device structure used was ITO/PEDOT:PSS (38 nm)/active layer/Ca (20 nm)/Al (100 nm) where the active layer was a solution-processed blend of the oligothiophene and the solubilised fullerene, $PC_{61}BM$. Details of device optimisation, including IPCE spectra, are given in the in ESI†. For compound **1**, an optimised power conversion efficiency of 2.25% was achieved when the film was spin-coated from a chlorobenzene solution as a 1 : 1 blend with $PC_{61}BM$. By contrast, the maximum power conversion efficiency obtained for a device based on compound **2** was 1.64%, when spun from chloroform (see Section 7.2 and 7.3 in ESI†). The current–voltage curves for the optimised blends of **1** and **2** with $PC_{61}BM$ are shown in Fig. 3.

Optimised devices based on compounds **1** and **2** showed open circuit voltages (V_{oc}) of 0.87 and 0.98 V respectively. These values are consistent with the measured HOMO values where the more positive HOMO for compound **1** would predict a lower V_{oc}. Devices based on compound **1** show a higher photocurrent than for compound **2**, a finding that is consistent with the observed red-shift in the absorbance for compound **1** compared with compound **2**.

The use of the C_{70} derivative of PCBM increased the V_{oc} of devices based on compound **1** slightly, but the overall PCE was, in contrast with other reports, comparable to the

Table 1 Photophysical and electrochemical properties of **1** and **2**

Dye	Absorption (solution) λ_{max}[a]/onset/nm [ε/(M^{-1} cm^{-1})]	Absorption (film) λ_{max}[b]/onset/nm	Emission (solution) λ_{max}[a]/nm	E_{HOMO} eV[c]	$E_{bandgap}$ eV[d]	E_{LUMO} eV[e]
1	590/722 [61 028]	584/790	800	−5.40	1.6	−3.8
2	514/636 [41 249]	544/728	716	−5.60	1.7	−3.9

[a] Absorption and emission spectra were measured in chloroform solution. [b] Absorption spectra of thin solid films spin-cast from chloroform solutions. [c] HOMO levels of the dyes were measured using Photo Electron Spectroscopy in Air (PESA) on thin solid films on glass. [d] Energy band gaps were estimated from the absorption onset in thin solid films. [e] LUMO levels were calculated from the optical band gaps and HOMO levels ($E_{LUMO} = E_{bandgap} + E_{HOMO}$).

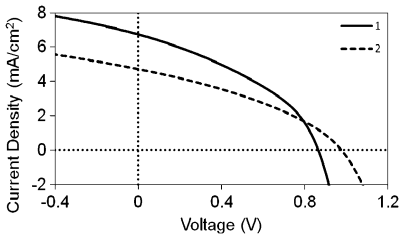

Fig. 3 Current–voltage curves for optimised devices based on **1** and **2** in blends with $PC_{61}BM$ (1 : 1 wt.) under simulated sunlight (AM1.5, 1000 W/m^2). Device Structure is: ITO/PEDOT:PSS (38 nm)/Active layer/Ca (20 nm)/Al (100 nm). For **1** the active layer was 46 nm thick, for **2** the active layer was 56 nm thick.

C_{60}-based devices (see Section 7.2 in ESI†). Improvements seen in using C_{70} are usually attributed to enhanced absorption in the film. Our results suggest that other factors, such as the low charge mobility or the film morphology, are the limiting factors in devices based on compound **1**. In particular, the modest fill factors observed for all devices suggest that the pathways for charges to the electrodes are not optimised, a problem that could be addressed by using donor fragments that encourage stronger intermolecular interactions.

With regards to the differences in processing conditions, it is noteworthy that, in contrast to compound **1**, devices based on compound **2** showed a significant drop in current when fabricated using a high boiling solvent. We[13] and others[2] have shown that this is a common issue for small molecule semiconductors where there is a need to limit the formation of large-scale crystals through the use of low boiling solvents. However, the use of low boiling solvents in printing processes is extremely problematic so the finding that compound **1** performs best when used with high boiling solvents is significant. AFM images of the active layer of devices show the finest morphology for the as-deposited films of compound **1** spun from chlorobenzene (see Fig. S7 and S8 in ESI†). Finally, with a view to printing devices under ambient conditions, we also conducted side-by-side comparisons of optimised devices fabricated in air and under inert conditions. While the differences were only minor, it was surprising that the best performing devices with compound **1** (PCE = 2.62%) were prepared in air with no annealing of either the PEDOT:PSS or the active layer (see section 7.5 in ESI†). Taken as a whole, these results strongly suggest that the solubilising group on the cyanopyridone acceptor reduces the tendency of the material to crystallise making it less dependent on processing conditions to deliver optimised devices. The coupling of this acceptor group with higher oligothiophenes is the subject of on-going work in our laboratories.

In conclusion, we have demonstrated the use of cyanopyridone to improve the performance of donor–acceptor small molecules in OPVs. In a direct comparison we have shown that this acceptor group lowers the band gap of an oligothiophene dye and, in devices, the cyanopyridone-functionalised compound shows higher device power conversion efficiency compared with an analogue containing a dicyanovinyl acceptor group. We have also shown that the solubilising alkyl group on the cyanopyridone fragment delivers a material that can be easily solution processed, that does not crystallise and that affords devices that can be fabricated with simple processes.

This research was funded through the Flexible Electronics Theme of the CSIRO Future Manufacturing Flagship and was also supported by the Victorian Organic Solar Cell Consortium (Victorian Department of Primary Industries, Sustainable Energy Research and Development Grant and Victorian Department of Business and Innovation, Victoria's Science Agenda Grant).

Notes and references

1 (*a*) G. Yu, J. Gao, J. C. Hummelen, F. Wudl and A. J. Heeger, *Science*, 1995, **270**, 1789–1791; (*b*) J. J. M. Halls, C. A. Walsh, N. C. Greenham, E. A. Marseglia, R. H. Friend, S. C. Moratti and A. B. Holmes, *Nature*, 1995, **376**, 498–500.
2 B. Walker, C. Kim and T.-Q. Nguyen, *Chem. Mater.*, 2011, **23**, 470–482.
3 J. L. Delgado, P.-A. Bouit, S. Filippone, M. Á. Herranza and N. Martín, *Chem. Commun.*, 2010, **46**, 4853–4865.
4 (*a*) G. D. Wei, S. Y. Wang, K. Sun, M. E. Thompson and S. R. Forrest, *Adv. Energy Mater.*, 2011, **1**, 184–187; (*b*) Y. Liu, X. Wan, F. Wang, J. Zhou, G. Long, J. Tian, J. You, Y. Yang and Y. Chen, *Adv. Energy Mater.*, 2011, **1**, 771–775.
5 J. E. Anthony, *Angew. Chem., Int. Ed.*, 2008, **47**, 452–483.
6 N. M. Kronenberg, M. Deppisch, F. Wurthner, H. W. A. Lademann, K. Deing and K. Meerholz, *Chem. Commun.*, 2008, 6489–6491.
7 N. M. Kronenberg, V. Steinmann, H. Bürckstümmer, J. Hwang, D. Hertel, F. Wurthner and K. Meerholz, *Adv. Mater.*, 2010, **22**, 4193–4197.
8 (*a*) A. B. Tamayo, X.-D. Dang, B. Walker, J. Seo, T. Kent and T.-Q. Nguyen, *Appl. Phys. Lett.*, 2009, **94**, 103301; (*b*) B. Walker, A. B. Tamayo, X.-D. Dang, P. Zalar, J. H. Seo, A. Garcia, M. Tantiwiwat and T.-Q. Nguyen, *Adv. Funct. Mater.*, 2009, **19**, 1–7.
9 S. Steinberger, A. Mishra, E. Reinold, C. M. Müller, C. Uhrich, M. Pfeiffer and P. Bäuerle, *Org. Lett.*, 2011, **13**, 90–93.
10 Y. Li, Q. Guo, Z. Li, J. Pei and W. Tian, *Energy Environ. Sci.*, 2010, **3**, 1427–1436.
11 (*a*) P. F. Xia, X. J. Feng, J. Lu, S.-W. Tsang, R. Movileanu, Y. Tao and M. S. Wong, *Adv. Mater.*, 2008, **20**, 4810–4815; (*b*) P. F. Xia, X. J. Feng, J. Lu, R. Movileanu, Y. Tao, J.-M. Baribeau and M. S. Wong, *J. Phys. Chem. C*, 2008, **112**, 16714–16720.
12 M. J. Frisch, *et al.*, *Gaussian 03, revision C.02*, Gaussian, Inc., Wallingford CT, 2004.
13 K. N. Winzenberg, P. Kemppinen, G. Fanchini, M. Bown, G. E. Collis, C. M. Forsyth, K. Hegedus, Th. B. Singh and S. E. Watkins, *Chem. Mater.*, 2009, **21**, 5701–5703.